UPDATED HIGH-ENERGY LHC DESIGN*

D. Amorim, S.A. Antipov, S. Arsenyev, M. Benedikt, R. Bruce, M. Crouch, S. Fartoukh,
M. Giovannozzi, B. Goddard, M. Hofer, J. Keintzel, R. Kersevan, V. Mertens, J. Molson,
Y. Muttoni, J. Osborne, V. Parma, V. Raginel, S. Redaelli, T. Risselada, I. Ruehl, B. Salvant,
D. Schoerling, E. Shaposhnikova, L. Tavian, E. Todesco, R. Tomás, D. Tommasini,
F. Valchkova-Georgieva, V. Venturi, D. Wollmann, F. Zimmermann†,
CERN, Geneva, Switzerland
A. Apyan, ANSL, Yerevan, Armenia; G. Guillermo, CINVESTAV Merida, Mexico
F. Burkart, DESY, Hamburg, Germany
J. Barranco, L. Mether, T. Pieloni, L. Rivkin, C. Tambasco, EPFL, Lausanne, Switzerland
J.L. Abelleira, E. Cruz-Alaniz, A. Seryi, L. van Riesen-Haupt, JAI Oxford, U.K.
A. Abramov, H. Pikhartova, JAI RHUL, Egham, U.K.; K. Ohmi, K. Oide, D. Zhou,
KEK, Tsukuba, Japan
Y. Cai, Y. Nosochkov, SLAC, Stanford, U.S.A.

Abstract

We present updated design parameters for a future High-Energy LHC. A more realistic turnaround time has led to a revision of the target peak luminosity, as well as a choice of a larger IP beta function, and longer physics fills. Pushed parameters of the Nb_3Sn superconducting cable together with a modified layout of the 16 T dipole magnets resulted in revised field errors, updated dynamic-aperture simulations, and an associated re-evaluation of injector options. Collimators in the dispersion suppressors help achieve satisfactory cleaning performance. Longitudinal beam parameters ensure beam stability throughout the cycle. Intrabeam scattering rates and Touschek lifetime appear benign.

INTRODUCTION

The HE-LHC would provide pp collisions at a centre-of-mass energy of 27 TeV, using the existing 26.7 km LHC tunnel infrastructure, and the same 16 T dipole magnets as being developed for the FCC-hh [1]. In contrast to the FCC-hh magnets, the HE-LHC magnets will be curved. Preliminary parameters of the HE-LHC were presented in [2]. A conceptual design report is being published [3]. Here we review the overall design. Arc optics, dynamic aperture, experimental insertions, and collimation for heavy ion beams are discussed in four companion papers [4–7].

OPTICS, LAYOUT & INJECTION

Two candidate arc optics for the HE-LHC were developed [2]. One of these is LHC-like with 23 cells per arc, and 90° phase advance per cell. The other optics features fewer (18), longer cells, which results in a larger dipole filling factor. The transition between arcs and dispersion-free straight sections is formed by a so-called dispersion suppressor (DS) [5]. In order for HE-LHC to fit into the existing

tunnel, the geometrical footprint of the HE-LHC must be matched to that of LEP or of the LHC. The offset in the arcs may generally be reduced to about 2 cm peak-to-peak [5]. However, the geometrical offset of the HE-LHC or LHC DS with respect to LEP depends on the total deflection of the 8 bends in each DS, whose strength and length could be adjusted individually.

After the LHC Injector Upgrade (LIU) [8], an extremely bright proton beam will be available. Injection into the HE-LHC could be accomplished from a new fast ramping superconducting (SC) synchrotron in the SPS tunnel (scSPS). SC magnets with double-layer coils would allow an injection energy of 1.3 TeV, which provides an adequate dynamic and physical aperture and has been chosen as a solid baseline. Alternative injector scenarios include injection at 900 GeV from a single-layer coil SC synchrotron in the SPS tunnel, or injection from the existing warm SPS at 450 GeV.

The nonlinear fields of the Nb_3Sn dipole magnets, due to persistent currents in the superconducting cable, limit the dynamic aperture at injection. To obtain an acceptable field quality, for the HE-LHC Nb_3Sn magnets, the effective filament size of the SC wire is chosen as 20 μm, which is smaller than the 50 μm filament diameter of the HL-LHC conductor. A further improvement is expected from the addition of Artificial Pinning Centres (APCs), with a realistic target value for the pinning efficiency taken to be 50%. Requiring a dynamic aperture above 12σ, as for the LHC design, and including the positive effect of magnet sorting, the injection energy must be at least 900 GeV [4].

OPERATION AND β^* CHOICE

The longitudinal emittance needs to be kept constant during the physics store, in order to maintain longitudinal Landau damping. On the other hand, the transverse emittance shrinks due to the strong radiation damping, while the proton intensity rapidly decreases. At the HE-LHC the proton burn-off time is comparable to the radiation damping time. This situation is qualitatively different from the LHC (where radi-

MC1: Circular and Linear Colliders

A01 Hadron Colliders

ation damping is negligible), HL-LHC (negligible radiation damping plus luminosity levelling) and FCC-hh (radiation damping faster than proton burn-off, also requiring transverse noise excitation to control beam-beam tune shift or pile-up), all discussed in [9]. At the HE-LHC, a partial luminosity levelling naturally occurs, since the emittance shrinks while the intensity decreases.

In 2017–2018, the LHC turnaround time was roughly 6 h on average [10, 11], and 3.5 h if not counting technical faults [12]. A similar turnaround time of about 5 h is assumed for the HE-LHC [13]. Such a figure appears attainable in view of the LHC experience and the planned HE-LHC ramp-up time of about 20 minutes [3]. We choose the β^* of the HE-LHC to be 45 cm, such that the optimum HE-LHC run time also becomes ~5 hours. At this value, both physical and dynamic aperture in collision are satisfactory [6].

COLLIMATION

With the reduced physical aperture at injection and smaller beams at higher energy, collimating the HE-LHC beams is more challenging than for the HL-LHC. As for the LHC and HL-LHC, the collimator system will be multi-staged, consisting of primary (TCP), secondary (TCSG), and tertiary collimators, plus others. The HE-LHC collimation design started from the HL-LHC layout [14], building on the well-tested LHC collimation system [15, 16]. Due to high beam losses in these regions, the LHC collimation straights in Interaction Region (IR) 7 (betatron collimation) and IR3 (momentum collimation) can only accommodate warm magnets. The HE-LHC design strategy has been to maintain or approximate the LHC optics with its carefully optimised collimator locations [17] and phase advances between collimators. Keeping exactly the same optics would have required a doubling of the integrated bending and focussing fields, which is not directly possible. However, minimising longitudinal gaps, eliminating any weakly excited quadrupoles and spare collimator slots, and increasing the length of all magnets to the maximum extent possible helped accomplish this goal approximately. For IR3 the remaining lack of integrated magnet strength in the region hosting the TCPs and TCSGs was compensated by length scaling, leading to beta function values that are increased by the same scaling factor. For IR7 such a length scaling was not necessary.

Like the HL-LHC, the HE-LHC will profit from DS collimators. The solution chosen for HL-LHC [14,18] can probably not be applied to the HE-LHC, since the standard dipole field is 16 T already. Instead we moved several dipoles to create space for collimators in DS cells 8 and 11, impacting the machine footprint.

The collimator hierarchy must be preserved in the presence of errors, which requires a minimum transverse distance of $1–2\sigma$ between the different levels of collimators, taking into account machine imperfections, optics and orbit stability, injection oscillations, and possible failure modes [19,20]. The HE-LHC collimator settings in units of σ are based on those for the HL-LHC. At top energy, the HE-LHC TCP

has a physical half gap of 0.82 mm, 40% smaller than the 1.2 mm of the HL-LHC TCP.

Figure 1 presents simulated cleaning inefficiencies in collision, using the setup of [16]. The local cleaning inefficiency is excellent, significantly less than 10^{-5}, for all cold sections (shown in blue, while losses in warm areas are displayed in red). An inefficiency of 7×10^{-6}/m would correspond to a local heat load of 10 mW/cm^3 for a 12 minute beam lifetime, to be compared with a quench limit of 100 mW/cm^3 [21]. The cleaning simulations also include two IR7 DS collimators set to about 18 and 22 σ. The DS collimators intercept practically all protons that otherwise would have been lost on the cold magnets in the DS. A similarly beneficial effect of DS collimators is seen for heavy ions [7].
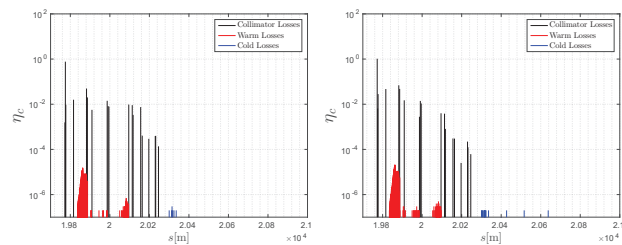

Figure 1: Simulated horizontal (left) and vertical cleaning inefficiency (right) around IR7 at collision energy with TCPs set at 6.7σ and TCSGs at 9.1σ. The simulation was performed with the code SixTrack [22, 23] using the scattering physics model of FLUKA [24].

Since for the HE-LHC the inter-beam separation in the arcs is increased to 250 mm, compared with 194 mm at the LHC, the necessity of the IR7/3 "dogleg" needs to be re-examined. Removing the dogleg dipoles would simplify the layout and optics of IRs 3 and 7.

LONGITUDINAL PARAMETERS

The requirement of longitudinal beam stability determines the minimum longitudinal emittance and RF voltages at all energies. Controlled emittance blow-up can be achieved by applying band-limited phase noise (as currently used in LHC operation). The emittance on the 13.5 TeV flat top is obtained by scaling from the value needed to ensure beam stability (Landau damping) at 7 TeV with the HL-LHC intensity (3 eVs), assuming the same effective impedance of $\mathrm{Im}(Z/n)_{\mathrm{eff}} = 0.11 \ \Omega$. For beam stability the longitudinal emittance must be varied as $\varepsilon_\| \propto E_b^{1/2}\gamma_t$. The RF voltage V_{RF} required for the same bucket filling factor scales with beam energy E_b, longitudinal emittance $\varepsilon_\|$, and gamma-transition as $V_{\mathrm{RF}} \propto \varepsilon_\|^2/(E_b\gamma_t^2)$. Therefore, the RF voltage is similar for different values of γ_t. The voltage of the 400 MHz RF system is about 11 MV, and the rms bunch length 9 cm, both at the injection energy of 1.3 TeV and at top energy [25]. In case, for the HE-LHC, $\mathrm{Im}(Z/n)_{\mathrm{eff}}$ increases by a factor F compared with the HL-LHC, the bunch length in physics would need to be approximately a factor $F^{1/5}$ longer. The RF power requirements do not exceed those of the HL-LHC.

COLLECTIVE EFFECTS

The direct space-charge tune shift of order 10^{-3} contributes to Landau damping of higher-order single-bunch head-tail modes [26]. The smaller chamber size will cause the indirect space charge effects to be enhanced compared to the LHC and HL-LHC. Extrapolating from [27], the vertical Laslett tune shift at 1.3 TeV will be about $\Delta Q_{\text{Laslett}} \approx -0.02$. Although the average tune shift can be corrected by adjusting the arc quadrupoles as a function of total beam intensity, some leakage of the AC magnetic field in the 10 kHz frequency range during filling of the machine could lead to noticeable bunch-to-bunch tune variation [27]. Another source of filling-pattern dependent bunch-to-bunch tune variation is the resistive-wall effect. Applying the results of [28] for the injection plateau, the resistive-wall transient could lead to a tune variation along the HE-LHC bunch trains of order 10^{-3}.

The intrabeam-scattering (IBS) emittance growth time at injection amounts to about 6–8 hours horizontally and 8–9 hours longitudinally [29]. Therefore, an emittance growth of about 5–6% longitudinally and 6–8% horizontally is expected to occur during 30 minutes at injection energy. This emittance growth could be reduced by means of a lower frequency RF capture system (e.g. 200 MHz), allowing for a larger longitudinal emittance and larger bunch length at injection. At top energy all IBS rise times exceed 25 hours; hence, they appear negligible compared with the radiation damping [29]. All Touschek lifetimes exceed 1000 h [29].

The impedance of the HE-LHC beamscreen in the cold arcs is larger than for the present LHC due to its smaller half aperture (12 versus ~18 mm in the vertical plane) and higher temperature (50 K for HE-LHC versus 5–20 K for LHC). However, the pumping holes are effectively shielded by the HE-LHC beamscreen [30]. The impedance for the room-temperature beam pipes is taken to be the same as for the LHC [31]. The collimators are a second major contributor to the transverse impedance budget. The HL-LHC collimation layout is considered, with primary (TCP) and secondary collimators (TCSG) in IR7 made from MoGr, without and with a 5 μm Mo coating, respectively [31]. The full HE-LHC impedance model (Fig. 2) also includes the broadband (BB) impedance and higher-order modes from the main RF cavities, plus contributions from four experiment vacuum chambers. Recombination chambers, shielded bellows, and arc BPMs are represented by a broadband resonator. Crab cavities are not included.

For instability estimates, the HL-LHC optics are assumed. At 1.3 TeV injection energy the HE-LHC requires a minimum damper gain equivalent to a damping time of 100 turns; the TMCI threshold is expected at a bunch population of 5×10^{11} protons, more than twice the design value [32].

PARAMETERS & OUTLOOK

Table 1 summarises the baseline design parameters. It is assumed that HE-LHC will accommodate two high-luminosity Interaction Points (IPs) 1 and 5, at the locations
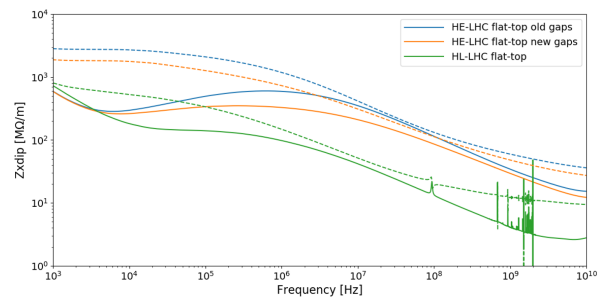

Figure 2: Real (solid curves) and imaginary part (dashed curves) of the HE-LHC transverse impedance at top energy compared with the HL-LHC transverse impedance and with an earlier HE-LHC impedance model featuring tighter collimator gaps [26], as a function of frequency [33].

of the present ATLAS and CMS experiments. For these experiments, an integrated pp luminosity exceeding 10 ab^{-1} is within reach over about 20 years of pp operation. IPs 2 and 8 could host secondary experiments combined with injection, as for the present LHC.

Table 1: HE-LHC Parameters for Operation with Protons

Parameter [unit]	HE-LHC
Centre-of-mass energy [TeV]	27
Injection beam energy [TeV]	1.3 (0.9)
Arc dipole field [T]	16
Beam current [A]	1.12
Bunch population N_b [10^{11}]	2.2
Bunch spacing [ns]	25
Longitudinal emittance ($\sim 4\pi\sigma_z\sigma_E$) [eVs]	4.2
Normalized transv. rms emittance $\gamma\varepsilon$ [μm]	2.5
IP1 & 5 beta function $\beta^*_{x,y}$ [m]	0.45
Peak luminosity in IP1 & 5 [10^{34} cm^{-2}s^{-1}]	16
Peak number of events / crossing	460
Synchrotron-radiation power / beam [kW]	100
Transverse emittance damping time τ [h]	3.6
Initial proton burn-off time τ_{bo} [h]	4.3
Luminosity per year (160 days) [fb^{-1}]	≥ 500

Like the LHC, the HE-LHC could also operate as a heavy-ion and ion-proton collider; and by adding a 60 GeV electron beam from an energy-recovery linac, the HE-LHC could provide lepton-proton and lepton-ion collisions [13].

The overall HE-LHC project schedule is dominated by accelerator and technology R&D, in particular by the time needed to develop and industrialise 16 T Nb$_3$Sn superconducting magnets. Another key input is the anticipated stop of HL-LHC. The HE-LHC programme will commence with a preparatory phase of 8 years, followed by the construction phase after the stop of the HL-LHC operation (dismantling of the existing SPS and LHC, civil engineering works and technical infrastructure, machines and detectors including commissioning) lasting 8 years. Then a period of 20 years

is needed to execute the currently envisaged physics programme. This makes a total of almost 30 years for construction and operation.

REFERENCES

[1] M. Benedikt *et al.*, "Future Circular Collider: Conceptual design report vol. 3", CERN-ACC-2018-0058, accepted for publication in *EPJ ST*, 2018.

[2] F. Zimmermann *et al.*, "High-Energy LHC Design", *J. Phys. Conf. Ser.*, vol. 1067, no. 2, p. 022009, 2018.

[3] F. Zimmermann *et al.*, "Future Circular Collider: Conceptual design report vol. 4", CERN-ACC-2018-005, accepted for publication in *EPJ ST*, 2018.

[4] M. Hofer, M. Giovannozzi, J. Keintzel, R. Tomás, F. Zimmermann, L. van Riesen-Haupt, "Dynamic Aperture at Injection for the HE-LHC", 10th International Particle Accelerator Conf. (IPAC'19), Melbourne, Australia, May 2019, paper MOPMP023, this conference.

[5] J. Keintzel *et al.*, "HE-LHC Optics Design Options", 10th International Particle Accelerator Conf. (IPAC'19), Melbourne, Australia, May 2019, paper MOPMP026, this conference.

[6] L. van Riesen-Haupt *et al.*, "Developments in the Experimental Interaction Regions of the High Energy LHC", 10th International Particle Accelerator Conf. (IPAC'19), Melbourne, Australia, May 2019, paper MOPMP039, this conference.

[7] A. Abramov *et al.*, "Collimation of Heavy Ion Beams in the HE-LHC", 10th International Particle Accelerator Conf. (IPAC'19), Melbourne, Australia, May 2019, paper MOPRB059, this conference.

[8] H. Damerau *et al.*, "LHC Injectors Upgrade, Technical Design Report, Vol. I: Protons", CERN-ACC-2014-0337, 2014.

[9] M. Benedikt, D. Schulte, F. Zimmermann, "Optimizing Integrated Luminosity of Future Hadron Colliders", *Phys. Rev. ST Accel. Beams*, vol. 8, p. 101002, 2015.

[10] B. Todd, L. Ponce, A. Apollonio, D. Walsh, "LHC Availability 2017: Standard Proton Physics", CERN-ACC-NOTE-2017-0063, 2017.

[11] B. Todd, L. Ponce, A. Apollonio, D. Walsh, "LHC Availability 2018: Proton Physics", CERN-ACC-NOTE-2018-0081, 2018.

[12] A. Apollonio, "LHC & Injectors Availability in Run 2", 9th LHC Operations Evian Workshop, Evian, 30 January – 1 February 2019, 2019.

[13] F. Bordry *et al.*, "Machine Parameters and Projected Luminosity Performance of Proposed Future Colliders at CERN", arXiv:1810.13022, CERN-ACC-2018-0037, 2018.

[14] G. Apollinari *et al.* (eds.), "High-Luminosity Large Hadron Collider (HL-LHC): Technical Design Report", CERN-2017-007-M, 2017.

[15] R.W. Assmann *et al.*, "The Final Collimation System for the LHC", in *Proc. EPAC'06*, Edinburgh, UK, Jun. 2006, paper TUODFI01, pp. 986–988.

[16] R. Bruce *et al.*, "Simulations and measurements of beam loss patterns at the CERN Large Hadron Collider", *Phys. Rev. ST Accel. Beams*, vol. 8, p. 081004, 2014.

[17] D.I. Kaltchev, M.K. Craddock, R.V. Servranckx, and J.B. Jeanneret, "Numerical Optimization of Collimator Jaw Orientations and Locations in the LHC", in *Proc. PAC'97*, Vancouver, Canada, May 1997, paper 7P026, pp. 153–155.

[18] R. Bruce, A. Marsili, and S. Redaelli, "Cleaning Performance with 11T Dipoles and Local Dispersion Suppressor Collimation at the LHC", in *Proc. IPAC'14*, Dresden, Germany, Jun. 2014, pp. 170–173. doi:10.18429/JACoW-IPAC2014-MOPRO042

[19] R. Bruce *et al.*, "Calculations of safe collimator settings and β^* at the CERN Large Hadron Collider", *Phys. Rev. ST Accel. Beams*, vol. 18, p. 061001, 2015.

[20] R. Bruce *et al.*, "Reaching record-low β^* at the CERN Large Hadron Collider using a novel scheme of collimator settings and optics", *Nucl. Instrum. Methods Phys. Res. A*, vol. 848, pp. 19–30, 2017.

[21] D. Tommasini and L. Bottura, private communications.

[22] F. Schmidt, "SIXTRACK: a single particle tracking code", Proc. Workshop on Nonlinear Problems in Future Particle Accelerators, Capri, Italy 1990, pp. 270–281 and CERN-SL-90-98-AP , 1990.

[23] SixTrack Code, http://sixtrack.web.cern.ch/SixTrack/

[24] T.T. Böhlen *et al.*, "The FLUKA Code: Developments and Challenges for High Energy and Medical Applications", *Nuclear Data Sheets*, vol. 120, pp. 211–214, 2014.

[25] E. Shaposhnikova, "Longitudinal beam parameters", informal HE-LHC Design Meeting, 25 July 2018, 2018.

[26] D. Amorim *et al.*, "Single-beam transverse collective effects for HE-LHC", *ICFA Beam Dyn. Newsl.*, vol. 72, p. 15100174, 2017.

[27] F. Ruggiero, "Single Beam Collective Effects in the LHC", *Particle Accelerators*, vol. 50, pp. 83–104, 1995.

[28] L. Vos, "Tune and Stability of High Intensity Bunch Trains in the CERN SPS and LHC", in *Proc. 7th European Particle Accelerator Conf. (EPAC'00)*, Vienna, Austria, Jun. 2000, paper WEP4A12, pp. 1176–1178.

[29] H. Pikhartova, "HE-LHC Touschek Lifetime and Intrabeam Scattering", HE-LHC Design Meeting no. 32, 31 July 2018, 2018. https://indico.cern.ch/event/747676/contributions/3092211

[30] S. Arsenyev, "Impedance aspects of the beam screen", HE-LHC Design Review, CERN, 11 December 2017, CERN, 11-12 Dec. 201, 2017. https://indico.cern.ch/event/674475/contributions/2805128

[31] D. Amorim *et al.*, "HL-LHC impedance and related effects," CERN-ACC-NOTE-2018-0087, 2018.

[32] S.A. Antipov, "Update on HE-LHC coherent beam stability from impedance", HE-LHC Design Meeting no. 36, 18 December 2018, 2018. https://indico.cern.ch/event/781175/contributions/3251366

[33] D. Amorim, "Update on the HE-LHC impedance model", HE-LHC Design Meeting no. 36, 18 December 2018, 2018. https://indico.cern.ch/event/781175/contributions/3251366